



The liquid crystal state: An intermediate state to obtain crystal packing

Loïc Leclercq^a, Andreea R. Schmitzer^{b,*}

^a Université Lille 1 and ENSCL, EA 4478 Chimie Moléculaire et Formulation, F-59655 Villeneuve d'Ascq Cedex, France

^b Université de Montréal, Département de Chimie, CP 6128 Succursale Centre-Ville, Montréal, Québec H3C 3J7, Canada



ARTICLE INFO

Article history:

Received 16 July 2014

Received in revised form 10 September 2014

Accepted 24 October 2014

Available online 30 October 2014

Keywords:

Imidazolium salts

Crystal growth

Liquid crystal

Hydrogen bonds

ABSTRACT

Two 1-alkyl-3-methylimidazolium trifluoromethanesulfonate, $[C_xMIM][TfO]$ ($x = 12$ or 20), form in appropriate solvents liquid crystal phases from which crystals can be obtained. The cohesion of this crystal is ensured by a combination of dispersion forces, H-bonds and electrostatic interactions developed firstly in the liquid crystal phase.

© 2014 Elsevier B.V. All rights reserved.

1. Introduction

Ionic liquids (ILs) constitute an attractive field in chemistry due to their solvent properties and the concept of “designer solvents” [1–3]. Indeed, the solvent properties of ILs should be able to be tailored to meet the requirements of specific applications, by varying the length and branching of the alkyl chains on the cationic and the anionic species. Imidazolium-based ILs were previously used as solvents in organic synthesis, organometallic catalysis, nanochemistry, electrochemistry, separation processes and as new materials [4–22], due to their unique physicochemical properties. Imidazolium unit can also be considered as a tecton because it possesses H-bonds donor through the three acidic protons localized on the cationic heterocyclic ring [23,24]. These H-bonds induce structural directionality contrary to classical salts in which the cohesion is mainly due to ionic bonds (Fig. 1a) [25–37]. Moreover, complementary electrostatic, π -stacking and van der Waals interactions can also occur in these salts (Fig. 1b) [38,39]. Therefore, in the solid state, the formation of the supramolecular networks is governed by molecular recognition processes between complementary tectons (i.e. cations and anions) leading to assembled units, and the long range translation of these units is leading to the formation of the 3D molecular networks. It is noteworthy that the strongest H-bonds always involves the most acidic proton H₂ followed by H₄ and H₅ of the imidazolium ring [40–42]. In the solid state, these H-bonds are weak to moderate but they act as complements of other interactions (electrostatic, van der Waals and π -stacking) [43]. There is a relationship between the liquid organization of ILs and the crystal structure. Indeed, the molecular packing and interactions in the first two or three

coordination shells is generally similar in both solid and liquid state [25]. To select or design imidazolium salts for a specific application, it is essential to understand the structure they will adopt in the liquid or solid phase. Several attempts have been made to predict the molecular packing in the solid phase [44,45]. However, this methodology is only valid for simple rigid structures where only small C–C rotation can occur [46]. Moreover, the crystallization of ILs with long alkyl tails (i.e. the surfactants based on ILs) is still an important challenge. Indeed, as pointed out by Drew Myers: “the packing of long hydrocarbon chains into a crystalline alignment is difficult because of the many possible variations in configuration for the units of the chain due to rotation about the four bonds to each carbon atom (rotational isomers). That difficulty is reflected in the relatively low melting points and poorly defined crystal structure of most hydrocarbons under normal conditions” [47]. On the other part, when water or other solvents are added to an imidazolium salt, the crystal structure can be partially disrupted to give a liquid crystal phase. This last possesses physical properties of both crystalline and fluid phases. Moreover, this phase has at least one highly ordered dimension [47]. We show herein that an intermediate organized liquid crystal phase can provide a good platform for the crystallization of these imidazolium salts. This new methodology can be applied for the crystallization of long alkyl chain length carried by an imidazolium ring and maybe to other surfactants.

2. Experimental section

2.1. Materials

All reactions were carried in oven-dried glassware under nitrogen, using standard Schlenk and vacuum line techniques. The ¹H and ¹³C NMR spectra were recorded on Advance 300 Bruker spectrometer at

* Corresponding author.

E-mail address: ar.schmitzer@umontreal.ca (A.R. Schmitzer).

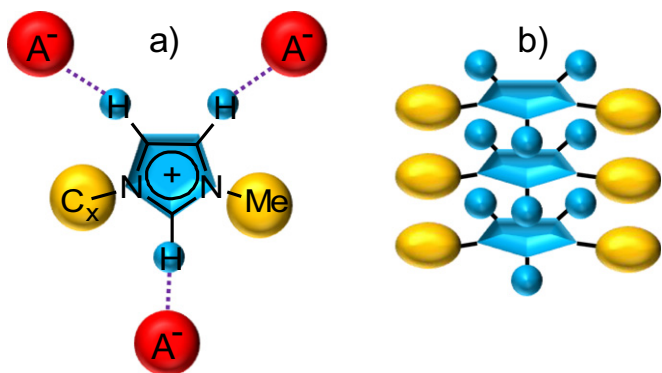


Fig. 1. Schematic representation of: a) the three H-bond donors (purple dotted line), and b) π -stacking interactions between imidazolium cations (blue pentagons) and triflate anions (red spheres).

300.13 and 75.49 MHz, respectively, with the samples nonspinning. Chemical shifts are given in ppm (δ) and measured relative to residual solvent. HR-MS analyses were obtained at the Université de Montréal facility. Trifluoromethanesulfonic anhydride was freshly prepared prior to use by distillation of a 1:1 w/w mixture of trifluoromethanesulfonic acid and phosphorus pentoxide. All other chemicals were purchased from Aldrich and used without further purification. “Distilled” solvents were obtained using a GlassContour system (Irvine, CA).

2.2. Synthesis of 1-alkyl-3-methylimidazolium triflate $[C_xMIM][TfO]$ with $x = 12$ or 20

A dry flask (250 mL), equipped with a magnetic stir bar and a septum-inlet for nitrogen, was charged with *n*-alkyl alcohol (5.4 mmol, 1 eq.) and poly(vinylpyridine) (1.15 eq.) in dichloromethane (50 mL). At 0 °C, trifluoromethanesulfonic anhydride (1.1 eq.) was dropwise added. The reaction mixture was stirred for 3 h to 0 °C at room temperature and then filtered under gravity. The poly(vinylpyridinium triflate) precipitate was washed with 5 mL of dichloromethane. The organic layer was washed with saturated NaHCO₃ solution and when the organic layer became transparency, we dried (MgSO₄) and concentrated under vacuum to give the *n*-alkyl triflate (yellowish oil). This oil was dissolved in anhydrous toluene under a nitrogen atmosphere and the solution was cooled to 0 °C. The 1-methylimidazole (1 eq.) was added and the resulting solution was stirred during 16 h at 57 °C. The ionic liquid layer appeared beneath the toluene phase or the ionic salt precipitated. The resulting salt was dried overnight at 120 °C under vacuum. The product was stored under dry nitrogen.

$[C_{12}MIM][TfO]$: Yield: 85%. m.p.: 40 °C. ¹H NMR (300 MHz, CDCl₃, 25 °C): δ = 0.87 (broad signal, 3H); 1.30 (broad signal, 18H); 1.90 (broad signal, 2H); 3.98 (s, 3H); 4.18 (t, 2H, ³J = 7.1 Hz); 7.31 (s, 1H); 7.39 (s, 1H); 9.13 (s, 1H). ¹³C NMR (75 MHz, CDCl₃, 25 °C): δ = 137.7; 124.5; 122.8; 119.6 (q, J_{CF} = 319.0 Hz); 51.0; 37.2; 32.7; 30.9; 30.4; 30.3; 30.1; 29.7; 26.9; 23.5; 14.9. HR-MS: *m/z* found: 251.2482 ($[C_{12}MIM]^+$), calc: 251.2487.

$[C_{20}MIM][TfO]$: Yield: 91%. m.p.: 76 °C. ¹H NMR (300 MHz, CDCl₃, 25 °C): δ = 0.88 (t, 3H); 1.28 (s, 34H); 1.83 (m, 2H); 3.98 (s, 3H); 4.18 (t, 2H); 7.27 (s, 1H); 7.29 (s, 1H); 9.14 (s, 1H). ¹³C NMR (75 MHz, CDCl₃, 25 °C): δ = 137.8; 124.4; 122.8; 121.0 (q, J_{CF} = 320.2 Hz); 51.0; 39.6; 37.2; 35.6; 32.7; 30.9; 30.7; 30.6; 30.6; 30.6; 30.4; 30.3; 30.2; 30.2; 29.8; 29.7; 27.0; 23.5; 14.9. HR-MS: *m/z* found: 363.3743 ($[C_{20}MIM]^+$), calc: 363.3739.

2.3. Crystallization and X-ray diffraction

Both imidazolium salts were submitted to different crystallization conditions, but any of these classical conditions did not allow obtaining

crystals. The imidazolium salt (1 g) was added to a water/ethanol solution (2.5 mL of each). The flask was sealed and placed in a thermoregulated bath. To obtain a crystallization of the imidazolium salt, the following temperature program was used: initial temperature 20 °C, ramp to 80 °C at 20 °C/min (until homogenization of the solution under stirring) and finally ramp to 20 °C at 0.5 °C/h (hold for 48 h). After a week (i.e. at the end of the temperature program), needles are obtained. A single crystal was mounted on a loop fiber. Data were collected using a Bruker microstar diffractometer equipped with a Platinum 135 CCD Detector, a Helios optics and a Kappa goniometer (Cu/K α radiation, 1.54178 Å, at 150 K). The crystal-to-detector distance was 4.0 cm, and the data collection was carried out in 512 × 512 pixel mode. The initial unit cell parameters were determined by a least-squares fit of the angular setting of strong reflections, collected by a 10.0 degree scan in 33 frames over three different parts of the reciprocal space (99 frames total). Due to geometrical constraints of the instrument and the use of copper radiation, we obtained consistently a data completeness lower than 100% in dependence of the crystal system and the orientation of the mounted crystal, even with appropriate data collection routines. Typical values for data completeness ranged from 83 to 92% for triclinic, 85–97% for monoclinic and 85–98% for all other crystal systems. The weighted R-factor wR and goodness of fit S were based on F², conventional R-factors R were based on F, with F set to zero for negative F². The threshold expression of F² > 2 σ (F²) was used only for calculating R-factors (gt) etc. and was not relevant to the choice of reflections for refinement. R-factors based on F² were statistically about twice as large as those based on F, and R-factors based on all data will be even larger.

3. Results and discussion

3.1. Synthesis and crystallization

3.1.1. Synthesis of imidazolium triflate salts

Our strategy of synthesis is based on the reaction of an intermediate (trifluoromethanesulfonic)acid ester with the 1-methylimidazolium. Indeed, *n*-alcohols can be easily converted into *n*-alkyl triflates in the presence of triflic anhydride and a non-nucleophilic base providing the expected intermediate, which is further reacted with the 1-methylimidazolium in dry toluene. Poly(4-vinylpyridin) was used in order to avoid the base alkylation and to facilitate the purification of 1-alkyl-3-methylimidazolium triflate salts ($[C_xMIM][TfO]$, with $x = 12$ or 20) [48]. Highly pure imidazolium triflates were isolated in excellent yields (>80%) and were characterized by ¹H and ¹³C NMR, and High Resolution Mass Spectrometry (HR-MS). All salts were kept in a glove box under argon atmosphere.

3.1.2. Crystallization in liquid crystal phase

The crystallization of pure imidazolium salts generally results in lamellar structures with alternating head-to-head and tail-to-tail arrangements. The energy of the crystal, as reflected by their fusion point (40 and 76 °C for $[C_{12}MIM]$ and $[C_{20}MIM]$, respectively), is governed by the nature of the salt. The salts with highly polar and small hydrophilic groups generally provide enhanced crystal stability. In contrast, the salts with long hydrocarbon chains provide a poor crystal packing due to a difficult crystalline alignment of the alkyl tails. Indeed, the flexibility of the alkyl chain provides a very important number of possible rotational isomers.

On the other hand, when water or other solvent was added to these long alkyl chain imidazolium salts, organized liquid crystalline phase were formed. A liquid crystalline phase can be described as a phase containing both specific molecular organization in a region surrounded by more liquid or amorphous regions. Therefore, the liquid crystalline phase can be seen as a prolific intermediate state to obtain pre-organization and initiate the crystallization process. In other words, the crystallization process goes through an initial pre-organization

state in the solvent, before forming crystals from which the solvent is excluded.

After several attempts, crystallizations were carried out efficiently from water/ethanol solutions. Thus, water/ethanol (1/1) solutions of each imidazolium triflate salt were heated until homogenization (80 °C) in order to accelerate the dissolution process. Then, the temperature was gradually decreased from 80 to 20 °C (0.5 °C/h) then left at 20 °C for 48 h. The solutions have been observed during a week using cross polarized optical microscopy (Fig. 2).

After the first heating (i.e. at 80 °C), we observed the absence of any birefringence. After 1 day at 68 °C, Maltese crosses were observed, suggesting the formation of a liquid crystalline phase. With the progressive decrease of the temperature, the number of Maltese crosses increased, as well as their sizes. At 32 °C (after 4 days), needles appeared in the liquid crystalline phase. Indeed, crystallization from the liquid crystal phase resulted in a highly oriented structure in which the molecules may possess extended chain morphology. After a week, the crystals were mounted on a loop fiber to perform X-rays diffraction.

3.2. Solid state analysis

3.2.1. Crystal information and structure of the cation

For [C₁₂MIM] [TfO], the displacement parameters are high for fluorine and oxygen atoms of the trifluoromethanesulfonate ions and the residual electronic densities at the end of the refinement are all located in the vicinity of O and F positions: this observation can point to some rotational disorder in the anion. The final R-factor (19.32%) indicates a very poor agreement between the observed and calculated intensities. In contrast, the [C₂₀MIM] [TfO] salt crystallizes in a triclinic system with *P* – 1 as space group and a disorder on the lateral eicosyl chain was observed due to little rotations of some C–C bonds (Tables 1 and 2).

No water or residual solvent molecules were present in the lattice, showing that the cohesion of the crystal is ensured only by the ionic components. Therefore, the asymmetric unit of the crystal structure is composed of two imidazolium cations and obviously two triflate anions. We used here the atom numbering of crystal by using the first digit of the atom's label as indication of the corresponding moiety (Fig. 3).

Table 1

Crystal, collection and refinement information for [C₂₀MIM] [TfO] crystal.^a

Crystal data			
Cation Formula	C ₂₄ H ₄₇ N ₂	β /deg	96.953 (2)
Anion Formula	CF ₃ SO ₃	γ /deg	96.814 (3)
Molecular weight	512.71	$V/\text{\AA}^3$	2814.98 (19)
Crystal system	Triclinic	<i>Z</i>	4
Space group	<i>P</i> – 1	Color	Colorless
<i>a</i> /\AA	9.4917 (4)	Crystal dim./mm	0.20 × 0.16 × 0.04
<i>b</i> /\AA	9.9553 (4)	μ/mm^{-1}	1.421
<i>c</i> /\AA	30.5188 (11)	Temperature/K	150
α /deg	97.017 (2)	$D_{\text{calc}}/\text{g}\cdot\text{cm}^{-3}$	1.210
Data collection and refinement			
<i>T</i> _{min}	0.718	$\theta_{\text{min}}/\text{deg.}$	1.47
<i>T</i> _{max}	0.945	$\theta_{\text{max}}/\text{deg.}$	67.95
Measured reflections	45,559	Limiting indices	$-9 \leq h \leq 10$
Independent reflections	8850		$-11 \leq k \leq 11$
Completeness to $\theta_{\text{max}}/\%$	86.3		$-36 \leq l \leq 36$
Data	8850	$\Delta\rho_{\text{min}}$ and $\Delta\rho_{\text{max}}/\text{e}\text{\AA}^{-3}$	-0.29 and 0.37
Parameters	843	Final <i>R</i> indices	<i>R</i> ₁ 0.0480
Restraints	4042	$[I > 2\sigma(I)]$	<i>wR</i> ₂ 0.1348
Goodness-of-fit on <i>F</i> ²	1.035	<i>R</i> indices (all data)	<i>R</i> ₁ 0.0605
<i>R</i> _{int}	0.034		<i>wR</i> ₂ 0.1427

^a Diffractometer: Bruker microstar equipped with a Platinum 135 CCD Detector, a Helios optics and a Kappa goniometer (Cu/K α radiation, 1.54178 \AA).

Table 2 reports the geometry of the cations obtained from the X-ray analysis.

3.2.2. Supramolecular assembly

The crystal structure reveals a typical organization compared to those previously observed for other imidazolium crystals, i.e. an extended 3-D network of imidazolium cations and triflate anions connected together by H-bonds [37]. In the present system, the H-bonds network is relatively weak according to published criteria. Indeed, as depicted in

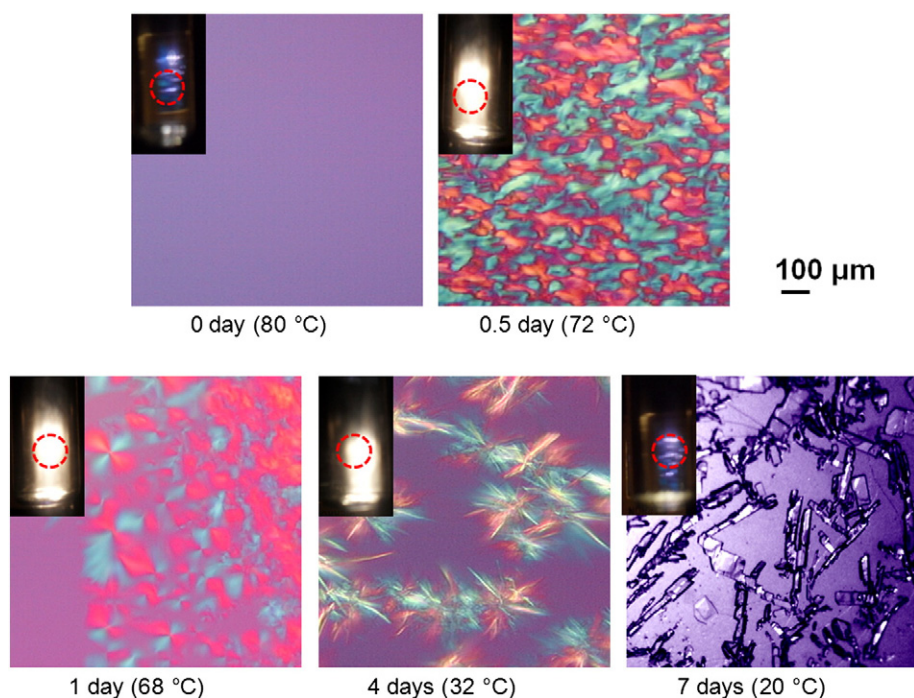


Fig. 2. Cross polarized optical microphotograph of water/ethanol (1/1) solutions of [C₂₀MIM] [TfO] salt as a function of time and temperature. The red circle shows the image of the polarization box.

Table 2
Experimental bond distances (Å), bond angles (\angle , °), and dihedral angles (D , °) of [C₂₀MIM] cations.

	X-rays diffraction	
	x = 1	x = 2
N _{x1} –C _{x2}	1.318 (3)	1.333 (2)
C _{x2} –N _{x3}	1.335 (2)	1.323 (2)
N _{x3} –C _{x4}	1.373 (3)	1.368 (2)
C _{x4} –C _{x5}	1.348 (3)	1.348 (3)
C _{x5} –N _{x1}	1.364 (3)	1.374 (2)
N _{x1} –CH _{x6}	1.467 (2)	1.469 (3)
N _{x3} –CH _{x7}	1.463 (3)	1.480 (2)
\angle N _{x1} –C _{x2} –N _{x3}	109.12 (18)	108.62 (15)
\angle N _{x3} –C _{x4} –C _{x5}	107.30 (17)	107.07 (17)
DN _{x1} –C _{x2} –N _{x3} –C _{x4}	1.0 (2)	–0.3 (2)
DC _{x2} –N _{x3} –C _{x4} –C _{x5}	–0.8 (2)	0.4 (2)
DC _{x2} –N _{x3} –C _{x7} –C _{x8}	–101.1 (5)	66.6 (5)
DC ₁₂ –N ₁₃ –C ₁₇ –C ₃₈	–109.5 (7)	–
DC ₁₂ –N ₁₃ –C ₁₇ –C ₅₈	–118.4 (6)	–
DC ₂₂ –N ₂₃ –C ₂₇ –C ₄₈	–	73.5 (9)
DC ₂₂ –N ₂₃ –C ₂₇ –C ₆₈	–	124.2 (5)
DC _{x7} –N _{x8} –C _{x9} –C _{x10}	–78.3 (1)	167.5 (12)
DC ₁₇ –N ₃₈ –C ₃₉ –C ₃₁₀	–75 (13)	–
DC ₁₇ –N ₃₈ –C ₅₉ –C ₅₁₀	73 (2)	–
DC ₂₇ –N ₄₈ –C ₄₉ –C ₄₁₀	–	170 (2)
DC ₂₇ –N ₄₈ –C ₆₉ –C ₆₁₀	–	–177 (2)

Table 3, the C–H \cdots Y (Y=O or F) distances are comprised between 2.2 and 2.8 Å and C–H \cdots Y angles between 112° and 174° [49–51]. The weakness of these H-bonds may be due to the steric hindrance of the triflate anions. However, the number of H-bonds compensates their weaknesses.

Each imidazolium cation is surrounded by three anions and vice versa. Overall, H-bonds, electrostatic interactions and the dispersion forces which operate between the alkyl tails are play the key role in the assembly of this ordered structure (Fig. 4). Finally, no π -stacking interactions can be observed in this structure due to the presence of the large triflate anions.

To get better insights in the molecular organization of the [C₂₀MIM] [TfO], we compared the structural organization of the salt with the [C₂MIM] [TfO] and [C₄MIM] [TfO] previously reported by Choudhury et al. (Fig. 5) [52,53]. It is important to note that the authors also reported at that time a phase transition for these short-chain imidazolium salts at very low temperatures.

Table 3
Distances (Å) and angles (°) of C–H \cdots Y hydrogen bonds in [C₂₀MIM] [TfO] crystal.

	C–H (Å)	H \cdots Y (Å)	C \cdots Y (Å)	C–H \cdots Y (°)
C ₁₂ –H ₁₂ –O ₂₂ ^a	0.95	2.4274	3.245 (3)	144.12
C ₁₄ –H ₁₄ –O ₂₁ ^b	0.95	2.3543	3.255 (2)	158.08
C ₁₅ –H ₁₅ –O ₁₃ ^c	0.95	2.5178	3.343 (3)	145.37
C ₁₆ –H _{16A} –O ₂₂ ^a	0.98	2.5760	3.466 (3)	151.03
C ₁₆ –H _{16C} –O ₁₁ ^b	0.98	2.5963	3.249 (3)	124.10
C ₁₇ –H _{17A} –O ₂₃ ^b	0.99	2.5825	3.552 (3)	166.35
C ₁₇ –H _{17B} –O ₁₂	0.99	2.4494	3.275 (3)	140.60
C ₁₇ –H _{17D} –O ₁₂	0.99	2.5431	3.275 (3)	130.64
C ₁₇ –H _{17E} –O ₁₂	0.99	2.5887	3.275 (3)	126.46
C ₁₇ –H _{17C} –O ₂₃ ^b	0.99	2.6326	3.552 (3)	154.56
C ₁₇ –H _{17E} –O ₂₃ ^b	0.99	2.7448	3.552 (3)	139.04
C ₂₂ –H ₂₂ –O ₁₁ ^d	0.95	2.2796	3.147 (2)	151.39
C ₂₄ –H ₂₄ –O ₂₃ ^e	0.95	2.6629	3.286 (3)	123.71
C ₂₅ –H ₂₅ –O ₁₃ ^d	0.95	2.5089	3.088 (2)	119.41
C ₂₆ –H _{26A} –O ₂₁ ^d	0.98	2.5417	3.242 (3)	128.33
C ₂₆ –H _{26B} –O ₁₂ ^f	0.98	2.4900	3.465 (2)	173.68
C ₂₇ –H _{27A} –O ₁₂ ^g	0.99	2.4341	3.372 (2)	157.96
C ₂₇ –H _{27E} –O ₁₂ ^g	0.99	2.4125	3.372 (2)	163.16
C ₂₇ –H _{27B} –O ₂₃ ^e	0.99	2.5433	3.363 (3)	140.09
C ₂₇ –H _{27C} –O ₂₃ ^e	0.99	2.6888	3.363 (3)	125.63
C ₂₇ –H _{27F} –O ₂₃ ^e	0.99	2.4935	3.363 (3)	146.42
C ₂₈ –H _{28A} –F ₁₃ ^d	0.99	2.6334	3.151 (12)	112.70
C ₄₈ –H _{48A} –F ₁₃ ^d	0.99	2.7728	3.293 (20)	113.36
C ₂₁₀ –H _{21B} –F ₂₂ ^h	0.99	2.4790	3.175 (10)	127.02
C ₄₁₀ –H _{41B} –F ₂₂ ^h	0.99	2.6614	3.417 (17)	133.33

Symmetry operators for Y:

- ^a 1 + x, –1 + y, z.
- ^b 1 + x, y, z.
- ^c 3 – x, 1 – y, 1 – z.
- ^d 1 – x, –y, 1 – z.
- ^e –x, 1 – y, 1 – z.
- ^f –1 + x, y, z.
- ^g 1 – x, –y, 1 – z.
- ^h 1 – x, 1 – y, 1 – z.

In these salts, cations and anions are typically connected by H-bonds between the acidic protons of the cation (H₂, H₄, H₅, N–CH₂– and N–CH₃) and the oxygen atom of the triflate anions. For [C₄MIM] [TfO], the H-bonds allow the formation of layers and each layer are head to tail in order to give weak hydrophobic interactions between two alkyl tails. Although the N-alkyl substituents are very different, the organization of [C₄MIM] [TfO] and [C₂₀MIM] [TfO] are very similar, suggesting that the dispersion forces are the driving forces of the crystallization process. In contrast, in the [C₂MIM] [TfO] crystal no dispersion forces between the alkyl tails of the two cations can be observed: the cohesion in

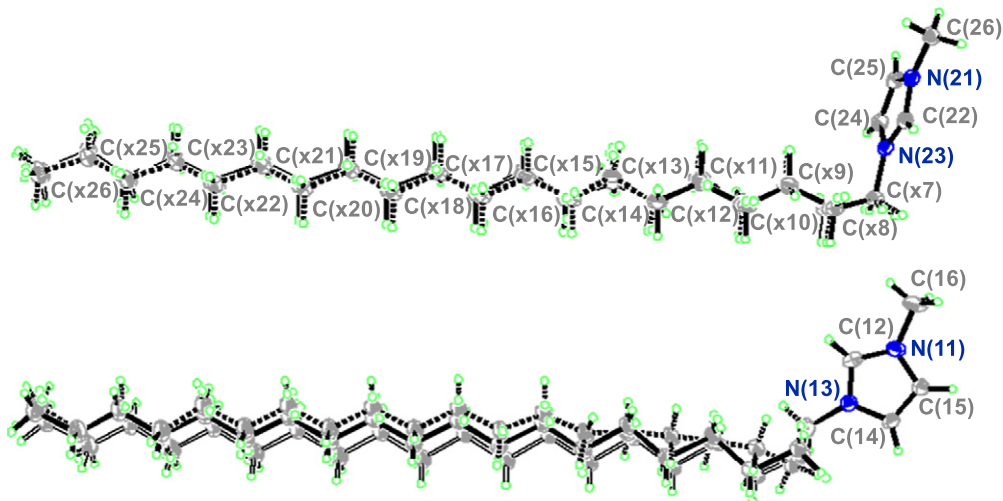


Fig. 3. ORTEP view of cations in the [C₂₀MIM] [TfO] crystal (for more details see ESI). Ellipsoids drawn at 30% probability level.

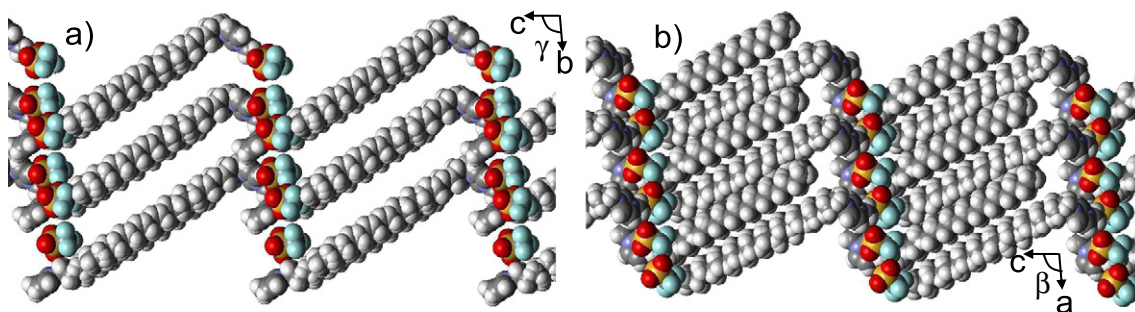


Fig. 4. Crystal packing of $[C_{20}MIM][TfO]$ salt obtained by X-ray diffraction: a) view down crystallographic a axis and b) view down crystallographic b axis.

this structure is essentially maintained by the H-bonds and electrostatic interactions.

4. Conclusion

Imidazolium ILs form in the solid state extended supramolecular networks of interconnected cations and anions. The dilution of these solid molecular networks in hot water/ethanol results in the disruption of the supramolecular network. However, when the temperature decreases, the separated ions form an intermediate liquid crystal phase

that allows the formation of crystals (Fig. 6). The crystallizations of 1-dodecyl- and 1-eicosyl-3-methylimidazolium triflate were performed from their intermediate liquid crystal phase. The crystallization process is probably favored for compounds possessing higher fusion temperatures, allowing to achieve a correct crystal packing. The structure of the cation, as well as the H-bonds, the electrostatic and the dispersion interactions govern the general packing and the lattice energy of these salts in the crystal. Fruitful developments could be probably made for the crystallization of other imidazolium salts and other ionic surfactants from a liquid crystal phase.

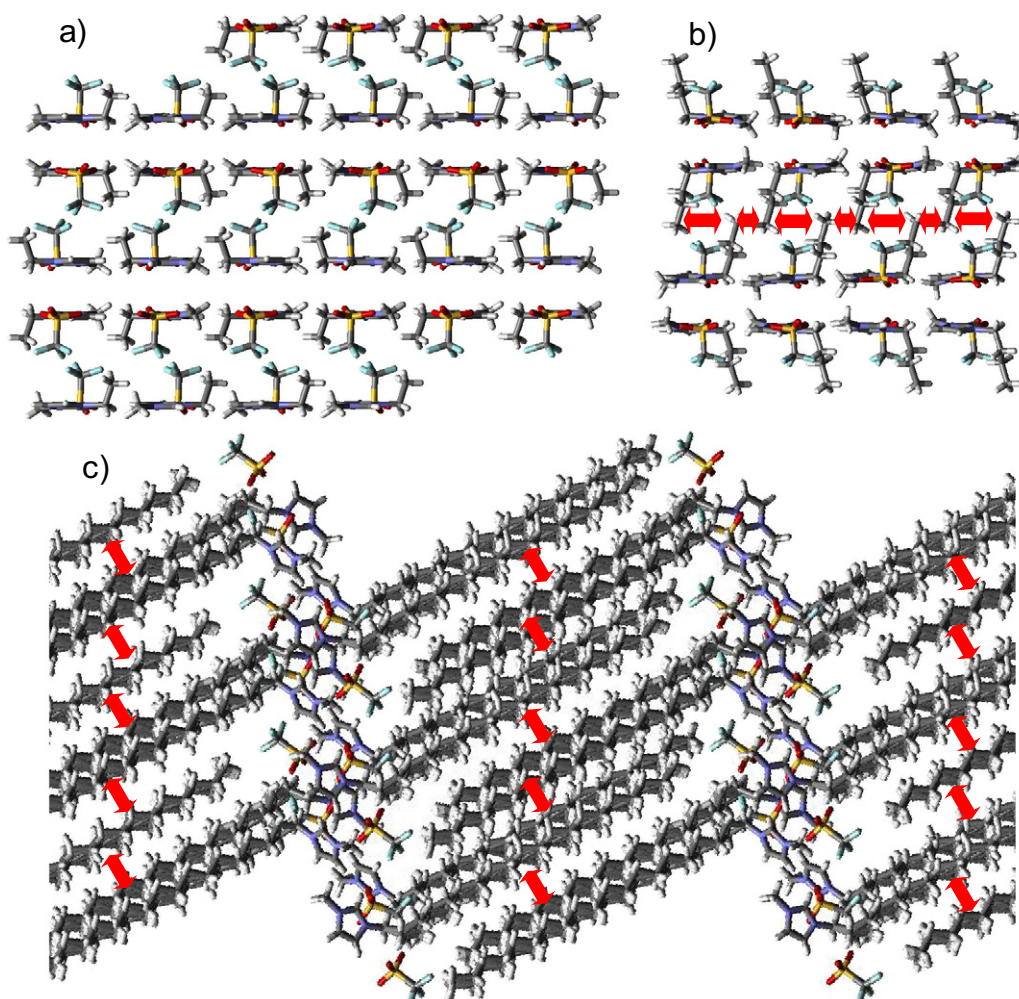


Fig. 5. Crystal packing of: a) $[C_2MIM][TfO]$, b) $[C_4MIM][TfO]$ and c) $[C_{20}MIM][TfO]$. The dispersion forces are shown as red double arrow.

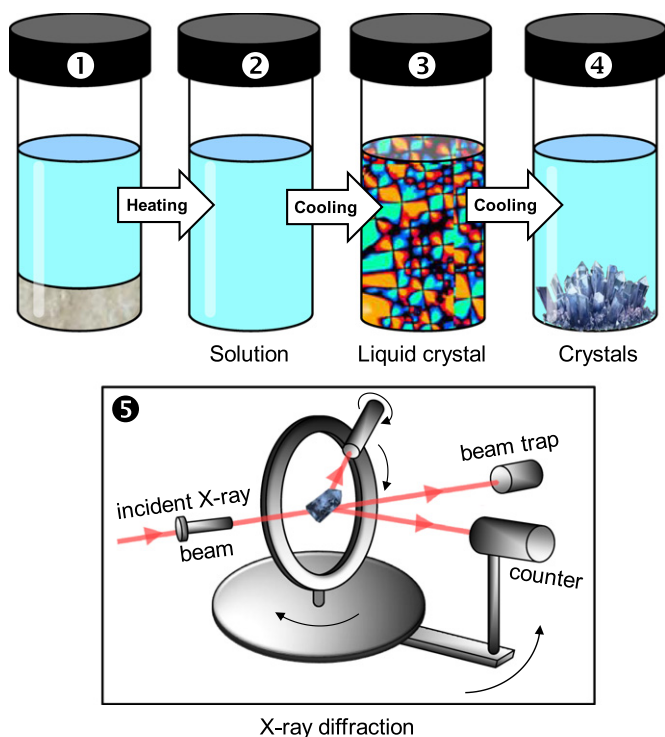


Fig. 6. Principle of the crystallization process in liquid crystal phase.

Appendix A. Supplementary data

Supplementary data associated with this article can be found in the online version, at <http://dx.doi.org/10.1016/j.molliq.2014.10.032>. CCDC-688096 contains the Supplementary crystallographic data for this paper. These data can be obtained free of charge from the Cambridge Crystallographic Data Centre via www.ccdc.cam.ac.uk/data_request/cif.

References

- [1] L. Leclercq, A.R. Schmitzer, *Supramol. Chem.* 21 (2009) 245.
- [2] N. Noujeim, L. Leclercq, A.R. Schmitzer, *Curr. Org. Chem.* 14 (2010) 1500.
- [3] P. Wasserscheid, T. Welton, *Ionic Liquids in Synthesis*, VCH-Wiley, Weinheim, 2002.
- [4] H. Zhao, S.V. Malhotra, *Aldrich. Acta* 35 (2002) 75.
- [5] Y. Chauvin, H. Olivier-Bourbigou, *Chemtech* 25 (1995) 26.
- [6] K.R. Seddon, *J. Chem. Technol. Biotechnol.* 68 (1997) 351.
- [7] K.R. Sheldon, *Chem. Commun.* (2001) 2399.
- [8] C. Baudequin, J. Baudoux, J. Levillain, D. Cahard, A.C. Gaumont, J.C. Plaquevent, *Tetrahedron Asymmetry* 14 (2003) 3081.
- [9] C.P. Mehnert, *Chem. Eur. J.* 11 (2005) 50.
- [10] H.-U. Blaser, M. Studer, *Green Chem.* 5 (2003) 112.
- [11] C.E. Song, *Chem. Commun.* (2004) 1033.
- [12] C.F. Poole, *J. Chromatogr. A* 1037 (2004) 49.
- [13] A.M. Stalcup, B. Cabovska, *J. Liq. Chromatogr. Relat. Technol.* 27 (2004) 1443.
- [14] S. Geetha, D.C. Trivedi, *Bull. Electrochem.* 19 (2003) 37.
- [15] M.J. White, F.J. Leeper, *J. Org. Chem.* 66 (2001) 5124.
- [16] M. Antonietti, D.B. Kuang, B. Smarsly, Z. Yong, *Angew. Chem. Int. Ed.* 43 (2004) 4988.
- [17] L. Leclercq, I. Suisse, F. Agbossou-Niedercorn, *Chem. Commun.* (2008) 311–313.
- [18] C. Pardin, L. Leclercq, A.R. Schmitzer, *Chem. Eur. J.* 16 (2010) 4686.
- [19] L. Leclercq, I. Suisse, G. Nowogrocki, F. Agbossou-Niedercorn, *Eur. J. Org. Chem.* 14 (2010) 2696.
- [20] S. Samsam, L. Leclercq, A.R. Schmitzer, *J. Phys. Chem. B* 113 (2009) 9493.
- [21] L. Leclercq, M. Lacour, S.H. Sanon, A.R. Schmitzer, *Chem. Eur. J.* 15 (2009) 6327.
- [22] C. Chiappe, D. Pieraccini, *J. Phys. Org. Chem.* 18 (2005) 275.
- [23] S. Mann, *Nature* 365 (1993) 499.
- [24] F.W. Fowler, J.W. Lauher, *J. Am. Chem. Soc.* 115 (1993) 5991.
- [25] J. Dupont, *Braz. Chem. Soc.* 15 (2004) 341.
- [26] A.G. Avent, P.A. Chaloner, M.P. Day, K.R. Seddon, T. Welton, *J. Chem. Soc. Dalton Trans.* (1994) 3405.
- [27] J. Dupont, P.A.Z. Suarez, R.F. de Souza, R.A. Burrow, J.P. Kintzinger, *Chem. Eur. J.* 6 (2000) 2377.
- [28] S. Saha, S. Hayashi, A. Kobayashi, H.-O. Hamaguchi, *Chem. Lett.* 32 (2003) 740.
- [29] D.G. Golovanov, K.A. Lyssenko, M.Y. Antipin, Y.S. Vygoskii, E.I. Lozinskaya, A.S. Shaplov, *CrystEngComm* 6 (2005) 53.
- [30] L. Leclercq, N. Noujeim, A.R. Schmitzer, *Cryst. Growth Des.* 9 (2009) 4784.
- [31] L. Leclercq, M. Simard, A.R. Schmitzer, *J. Mol. Struct.* 918 (2009) 101.
- [32] N. Noujeim, S. Sanon, L. Eberlin, A.R. Schmitzer, *Soft Materials* 8 (2012) 10914–10920.
- [33] A. Downard, M.J. Earle, C. Hardacre, S.E.J. McMath, M. Nieuwenhuyzen, S. Teat, *J. Chem. Mater.* 16 (2004) 43.
- [34] J.D. Holbrey, W.M. Reichert, R.D. Rogers, *Dalton Trans.* 15 (2004) 2267.
- [35] T. Fujimoto, M. Kawahata, Y. Nakakoshi, K. Yamaguchi, T. Machinami, K. Nischikawa, M. Tashiro, *Anal. Sci.* 23 (2007) 107.
- [36] Y. Nakakoshi, M. Shiro, T. Fujimoto, T. Machinami, H. Seki, M. Tashiro, K. Nischikawa, *Chem. Lett.* 35 (2006) 1400.
- [37] J. Dupont, P.A.Z. Suarez, *Phys. Chem. Chem. Phys.* 8 (2006) 2441.
- [38] L. Leclercq, A.R. Schmitzer, *J. Phys. Chem. A* 112 (2008) 4996.
- [39] H. Zhang, H. Liang, J. Wang, K. Li, *Z. Phys. Chem.* 221 (2007) 1061.
- [40] T.L. Amyes, S.T. Diver, J.P. Richard, F.M. Rivas, K. Toth, *J. Am. Chem. Soc.* 126 (2004) 4366.
- [41] R.W. Alder, P.R. Allen, S.J. Williams, *J. Chem. Soc. Chem. Commun.* 1267 (1995).
- [42] F.G. Bordwell, A.V. Satish, *J. Am. Chem. Soc.* 113 (1991) 985.
- [43] G.A. Jeffrey, *An Introduction to Hydrogen Bonding*, Oxford University Press, Oxford, 1997.
- [44] L. Leclercq, I. Suisse, G. Nowogrocki, F. Agbossou-Niedercorn, *Green Chem.* 9 (2007) 1097–1103.
- [45] L. Leclercq, I. Suisse, G. Nowogrocki, F. Agbossou-Niedercorn, *J. Mol. Struct.* 892 (2008) 433.
- [46] L. Leclercq, A.R. Schmitzer, *Cryst. Growth Des.* 11 (2011) 3828.
- [47] D. Myers, *Surfactant Science and Technology*, Wiley-Interscience, Hoboken, 2006, 113.
- [48] L. Leclercq, I. Suisse, P. Roussel, F. Agbossou-Niedercorn, *J. Mol. Struct.* 1010 (2012) 152.
- [49] P.B. Hitchcock, K.R. Seddon, T. Welton, *J. Chem. Soc. Dalton Trans.* (1993) 2639.
- [50] C.M. Gordon, J.D. Holbrey, A.R. Kennedy, K.R. Seddon, *J. Mater. Chem.* 8 (1998) 2627.
- [51] F.R. Desiraju, *Crystal Design: Structure and Function; in Perspectives in Supramolecular Chemistry*, Wiley, Chichester, 2004.
- [52] A.R. Choudhury, N. Winterton, A. Steiner, A.I. Cooper, K.A. Johnson, *CrystEngComm* 8 (2006) 742.
- [53] A.R. Choudhury, N. Winterton, A. Steiner, A.I. Cooper, K.A. Johnson, *J. Am. Chem. Soc.* 127 (2005) 16792.